

EMD APPROACH TO MULTICHANNEL EEG DATA — THE AMPLITUDE AND PHASE COMPONENTS CLUSTERING ANALYSIS

TOMASZ M. RUTKOWSKI

*Laboratory for Advanced Brain Signal Processing,
RIKEN Brain Science Institute, 2-1 Hirosawa, Wako-shi,
Saitama 351-0198, Japan
tomek@brain.riken.jp*

DANILO P. MANDIC

*Communication and Signal Processing Research Group,
Department of Electrical and Electronic Engineering,
Imperial College, Exhibition Road, London,
SW7 2BT, United Kingdom
d.mandic@imperial.ac.uk*

ANDRZEJ CICHOCKI

*Laboratory for Advanced Brain Signal Processing,
RIKEN Brain Science Institute,
2-1 Hirosawa, Wako-shi, Saitama 351-0198, Japan
cia@brain.riken.jp*

ANDRZEJ W. PRZYBYSZEWSKI

*Department of Neurology,
University of Massachusetts Medical School, MA, USA
Andrzej.Przybyszewski@umassmed.edu*

Human brains exhibit a possibility to control directly the intelligent computing applications in form of brain computer/machine interfacing (BCI/BMI) technologies. Neurophysiological signals and especially electroencephalogram (EEG) are the forms of brain electrical activity which can be easily captured and utilized for BCI/BMI applications. Those signals are unfortunately usually very highly contaminated by external noise caused by the presence of different devices in the environment creating electromagnetic interference. In this paper, we first decompose each of the recorded channels, in multichannel EEG recording environment, into intrinsic mode functions (IMF) which are a result of empirical mode decomposition (EMD) extended to multichannel analysis. We present novel and interesting results on human mental and cognitive states estimation based on analysis of the above-mentioned stimuli-related IMF components. The IMF components are further clustered for their spectral similarity in order to identify only those carrying responses to present stimuli to the subjects. The resulting targets only

reconstruction allows us to identify when and to which stimuli intelligent application user is tuning at a time.

Keywords: Brain synchrony; brain signal processing; EMD application to EEG.

1. Introduction

Online brain states analysis based on noninvasive monitoring techniques such as electroencephalogram (EEG) have received much attention recently due to the growing interest and popularity of research related to brain computer/machine interfacing (BCI/BMI) techniques, owing to the very exciting possibility of computer-aided communication with the outside world. A new and growing interest in neuroscience, so-called steady-state potentials^{1–3} stimuli technique, which produces longer in-time and more easy to detect within monitored EEG steady responses contributes also to EEG signal processing's recent popularity.

EEG based brain stages monitoring is achieved in a noninvasive recording setup. The noninvasive brain monitoring method possesses several important and difficult problems. In terms of signal processing these include the detection, estimation, interpretation and modeling of brain activities, and cross-user transparency.⁴

It comes as no surprise, therefore, that this technology is envisaged to be at the core of future “intelligent computing”. Other industries which would benefit greatly from the development of online analysis and visualization of brain states include the prosthetics, entertainment, virtual reality, and computer games industries, where the control and navigation in a computer-aided application is achieved without resorting to using muscles, hands, or any gestures (peripheral nervous system in general). Instead, the onset of “planning an action” recorded from the head (scalp) surface, and the relevant information is “decoded” from this information carrier.

Apart from purely signal conditioning problems, in most BCI/BMI experiments other issues such as user training and adaptation, inevitably cause difficulties and limit a wide spread of this technology due to the lack of “generality” caused by cross-user differences.⁴ To help mitigate some of the above-mentioned issues, we propose to make use of a new and growing interest in signal processing community technique of empirical mode decomposition (EMD)⁵ which we extend to multichannel approach of parallel decomposition of single channel signals and further clustering of so-obtained components among channels to track coherent (synchronized or correlated in spectral domain) activities in complex signals as EEG.

In the proposed approach, we analyze responses from experiments based on a visual stimuli which were conducted with in the Laboratory for Advanced Brain Signal Processing, BSI RIKEN, within the so-called steady-state visual evoked potential (SSVEP) mode.^{1,6} Within this framework, the subjects are asked to focus their attention on a simple flashing stimuli, whose frequency is known to cause a physiologically stable response traceable within EEG.^{6,7} This way, the proposed multichannel and multimodal signal decomposition scheme uses the EEG captured

by several electrodes, subsequently preprocessed, and transformed into informative time–frequency traces, which very accurately visualize frequency and amplitude modulations of the original signal.

EEG is usually characterized as a summation of extracellular currents caused by post-synaptic potentials (intracellular) from a very large number of neurons which create oscillatory patterns distributed and possible to record around the scalp. Those patterns in the known frequency ranges can be monitored and classified in synchrony with a stimuli given to the subjects. EMD utilizes empirical knowledge of oscillations intrinsic to a time series in order to represent them as a superposition of components with well defined instantaneous frequencies. These components are called intrinsic mode functions (IMF).

This paper is organized as follows. First the method of single channel EMD analysis of EEG signals is presented. Next multichannel EEG analysis and decomposition is discussed leading to a novel time–frequency synchrony evaluation method based on spectral IMF clustering. A new concept of multiple spatially localized amplitude and frequency oscillations related to presented stimuli in time–frequency domain is described which let us obtain final traces of frequency and amplitude ridges coherent among the EEG channels. Finally examples of the analysis of the EEG signals are given and conclusions are drawn.

2. Methods

We aim at looking at the level of detail (richness of information source) obtainable from single experimental trial EEG signals, and compare the usefulness of a novel multi-channel signal decomposition approach in this context. The utilized approach is based on multichannel extension of the EMD technique which was previously successfully applied to EEG sonification and mental states estimation in Refs. 1–3. The EMD approach rests on the identification of signal’s nonstationary and nonlinear features which represent different modalities of brain activity captured by the EEG data acquisition system (g.USBamp[®] of Guger Technologies). This novel method allowed us previously to create slowly modulated tones representing changing brain activities among different human scalp locations where EEG electrodes were localized.

In the current application, we propose to look at the level of details revealed in single EEG channels decomposed separately into IMFs as discussed in detail in the next section and later compared across the multiple channels. After application of Hilbert transform to all IMFs we can track and visualize revealed oscillations of amplitude and frequency ridges. Similarity of these oscillations among channels revealed in form of pairwise correlations identify components which are synchronized or not with the onsets and offsets of the presented stimuli. The proposed approach is a completely “data driven” concept. All the IMFs create semi-orthogonal bases created from the original EEG signals and not introduced artificially by the method itself.

2.1. EMD for EEG analysis — A single channel case

The IMF components obtained during EMD analysis should approximately obey the requirements of

- (i) completeness;
- (ii) orthogonality;
- (iii) locality;
- (iv) adaptiveness.⁵

To obtain an IMF it is necessary to remove local riding waves and asymmetries, which are estimated from local envelope of minima and maxima of the waveform. There are several approaches to estimate signals envelopes and we have discussed them previously.³

The Hilbert spectrum for a particular IMF allows us later to represent the EEG in amplitude — instantaneous frequency — time plane. An IMF shall satisfy the two conditions:

- (i) in the whole dataset, the number of extrema and the number of zero crossings should be equal or differ at most by one;
- (ii) at any point of IMF the mean value of the envelope defined by the local maxima and the envelope defined by the local minima should be zero.

The technique of finding IMFs corresponds thus to finding limited-band signals. It also corresponds to eliminating riding waves from the signal, which ensures that the instantaneous frequency will not have fluctuations caused by an asymmetric waveform. IMF in each cycle is defined by the zero crossings. Every IMF involves only one mode of oscillation, no complex riding waves are thus allowed. Notice that the IMF is not limited to be a narrow band signal, as it would be in traditional Fourier or wavelets decomposition, in fact, it can be both amplitude and frequency modulated at once, and also nonstationary or nonlinear.

The process of IMF extraction from a signal $x(t)$ (“sifting process”⁵) is based on the following steps:

- (1) determine the local maxima and minima of the analyzed signal $x(t)$;
- (2) generate the upper and lower signal envelopes by connecting those local maxima and minima, respectively, by the chosen interpolation method (e.g., linear, spline, cubic spline, piece-wise spline^{3,5});
- (3) determine the local mean $m(t)$, by averaging the upper and lower signal envelopes;
- (4) subtract the local mean from the data:

$$h_1(t) = x(t) - m_1(t). \tag{1}$$

Ideally, $h_1(t)$ is an IMF candidate. However, in practice, $h_1(t)$ may still contain local asymmetric fluctuations, e.g., undershoots and overshoots; therefore, one needs to repeat the above four steps several times, resulting eventually in the first (optimized) IMF. In order to obtain the second IMF, one applies the sifting process to the residue

$$\varepsilon_1(t) = x(t) - \text{IMF}_1(t), \quad (2)$$

obtained by subtracting the first IMF from $x(t)$; the third IMF is in turn extracted from the residue $\varepsilon_2(t)$ and so on. One stops extracting IMFs when two consecutive sifting results are close to identical; the EMD of the signal $x(t)$ may be written as:

$$x(t) = \sum_{k=1}^n \text{IMF}_k(t) + \varepsilon_n(t), \quad (3)$$

where n is the number of extracted IMFs, and the final residue $\varepsilon_n(t)$ can either be the mean trend or a constant. The EMD is obviously complete, since Eq. (3) is an equality: the original signal can be reconstructed by adding all IMFs and the final residue. Note that the IMFs are not guaranteed to be mutually orthogonal, but in practice, they often are close to orthogonal³; it is also noteworthy that the IMFs are adaptive, i.e., they depend on the signal $x(t)$ as anticipated for the data driven method.

2.2. Huang–Hilbert spectra with amplitude and frequency ridges

From the obtained in previous section IMFs corresponding time–frequency representations can be produced by applying the Hilbert transform to each component.⁵ As a result of Hilbert transform application to each IMF the data can be expressed as time–frequency domain in form of analytic complex signals formed as

$$\text{IMF}_{k,\text{an}}(t) = \text{IMF}_k(t) + i\text{IMF}_{k,\text{HT}}(t) = \text{IMF}_k(t) + \frac{1}{\pi} \int_{-\infty}^{+\infty} \frac{\text{IMF}_k(t')}{t - t'} dt', \quad (4)$$

where IMF_{HT} is the Hilbert transformed version of IMF. The analytic signal is further polar-decomposed as

$$\text{IMF}_{k,\text{an}}(t) = A_{\text{IMF}_k}(t) \exp(i\phi_{\text{IMF}_k}(t)), \quad (5)$$

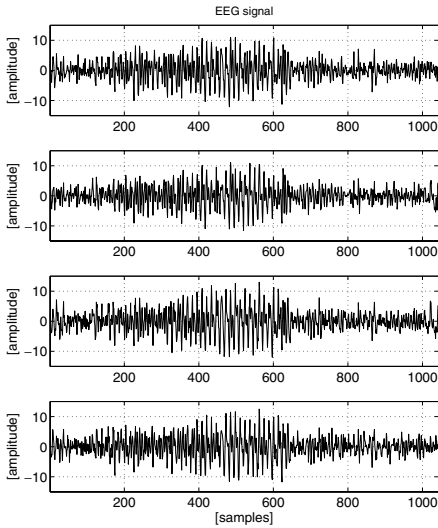
where

$$A_{\text{IMF}_k}(t) = \sqrt{\text{IMF}_k(t)^2 + \text{IMF}_{k,\text{HT}}(t)^2} \quad (6)$$

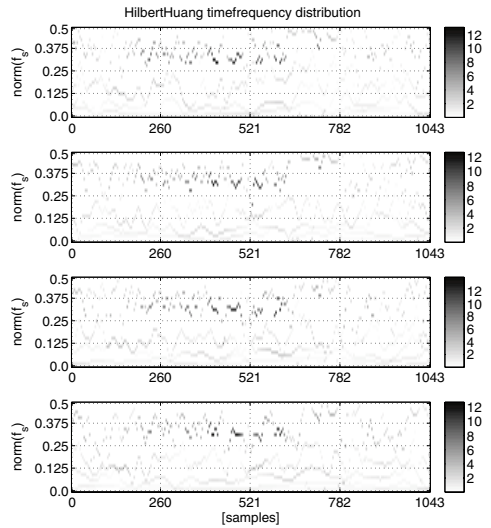
is the instantaneous amplitude, and

$$\phi_{\text{IMF}_k}(t) = \arctan\left(\frac{\text{IMF}_{k,\text{HT}}(t)}{\text{IMF}_k(t)}\right) \quad (7)$$

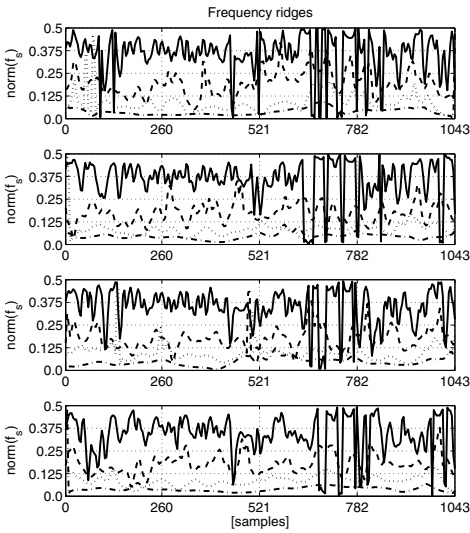
is instantaneous phase of each IMF_k , respectively. The Hilbert transform allows us to depict the variable amplitude (Fig. 1(d)) and the instantaneous frequency (Fig. 1(c))



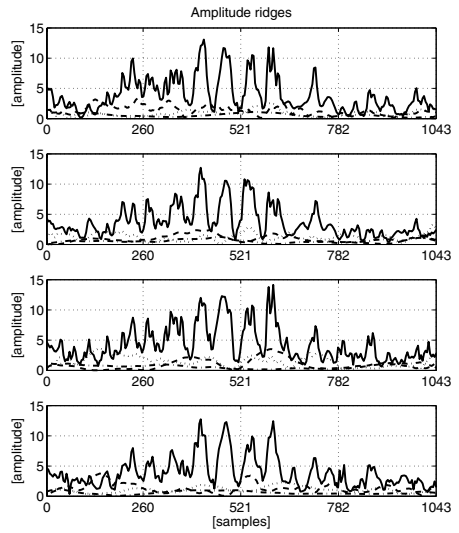
(a) Time domain preprocessed EEG.



(b) Huang–Hilbert spectra.



(c) Frequency ridge traces.



(d) Amplitude ridge traces

Fig. 1. Four plots of four EEG channels in each panel recorded synchronously during SSVEP experiment. The steady-state response can be visually spotted in the range of 150–650 samples. Panel (a) presents time domain EEG preprocessed plots; (b) their Huang–Hilbert spectra; (c) and (d) the frequency and amplitude ridges in Hilbert spectra domain (solid line: first; dashed line: second; dotted line: third; dash-dotted line: fourth IMF, respectively).

in the form of very sharp and localized functions of frequency and time (in contrast to Fourier expansion, for example, where frequencies and amplitudes are fixed for its bases). Such an approach is very suitable for the nonstationary EEG analysis and common/synchronized activities within certain channels. An example of Huang–Hilbert spectrograms of four EEG channels recorded simultaneously is presented in Fig. 1(b).

2.3. EMD application to multichannel EEG signals

Using the above procedure in a single channel mode the EEG signals from chosen electrodes could be decomposed separately forming subsets of IMF functions, from which low frequency drifts and high frequency spikes could be further removed. The most interesting part of EEG is usually in the middle range frequencies. To analyze multichannel EEG signal sets recorded synchronously in a single experiment we propose to decompose all channels separately preventing possible oscillatory information leaking among the channels. The so-obtained IMFs sets can be further compared as in case of four EEG signals presented in Fig. 1(a) which are further EMD decomposed and visualized in form of Huang–Hilbert spectrograms⁵ as in Fig. 1(b). The traces of amplitude and frequency modulation ridges⁸ obtained from Hilbert transformation of separately processed IMFs and further plotted together are presented in Figs. 1(d) and 1(c), respectively. Ridges are the continuous traces within spectrograms of frequency and amplitude oscillations as first introduced in Ref. 8. The areas of steady-state stimulation can be easily spotted in amplitude traces of a single IMF on all channels in Fig. 1(d) and subsequently in form of stable frequency ridge during stimulation with very strong oscillations before and after the stimuli in all channels as in Fig. 1(c).

The combined result of analysis of seven EEG channels from locations around the human head during similar SSVEP stimuli BCI/BMI paradigm is shown also in Fig. 5. There are seven time domain EEG traces plotted with only two amplitude (AR) and frequency (FR) ridges of the only components showing synchrony with the stimuli. Those components were obtained based on spectral clustering technique and thresholding described in the next section.

2.4. Spectral clustering of EMD components

In order to compare all IMFs extracted from the analyzed channels we propose to transform them to Hilbert domain in order to capture spectral content carried by all of them. The spectra are further treated as feature vectors and compared for their similarity across the channels.

We decided to compare several distance measures in order to test their usability for IMF components clustering resulting in EEG interference separation from the signals.

The distances were evaluated in form of a hierarchical cluster analysis using a set of dissimilarities for the n objects to be clustered. Such a procedure was performed⁹ with utilization of “R” package.¹⁰ Initially, each vector representing power spectrum values is assigned to its own cluster and then the algorithm proceeds iteratively, at each stage joining the two most similar clusters. The procedure continues until there is just a single cluster. At each stage distances between clusters are recomputed by the Lance–Williams dissimilarity update formula with a single linkage clustering method. The single linkage method is closely related to the minimal spanning tree concept and it adopts a “friends of friends” strategy for clustering.⁹ Results of such procedure are presented in Figs. 2(a), 2(b), 3(a), 3(b), 4(a), and 4(b), where two sets of clusters are visualized. The following distance measures were tested (written here for two vectors x and y):

2.4.1. Euclidean distance

The Euclidean distance is a usual square distance between the two vectors (two-norm). A result of clustering with this measure (not very good though with most of the IMFs clustered together) is presented in Fig. 2(a).

2.4.2. Maximum distance

The maximum distance is calculated as a maximum distance between two components of x and y (supremum norm). A result of clustering with this measure (here also most of the IMFs created a single cluster) is presented in Fig. 2(b).

2.4.3. Manhattan distance

The Manhattan distance is based on an absolute distance between the two vectors (one-norm). A result of clustering with this measure (here again most of the IMFs created a single cluster) is presented in Fig. 3(a).

2.4.4. Canberra distance

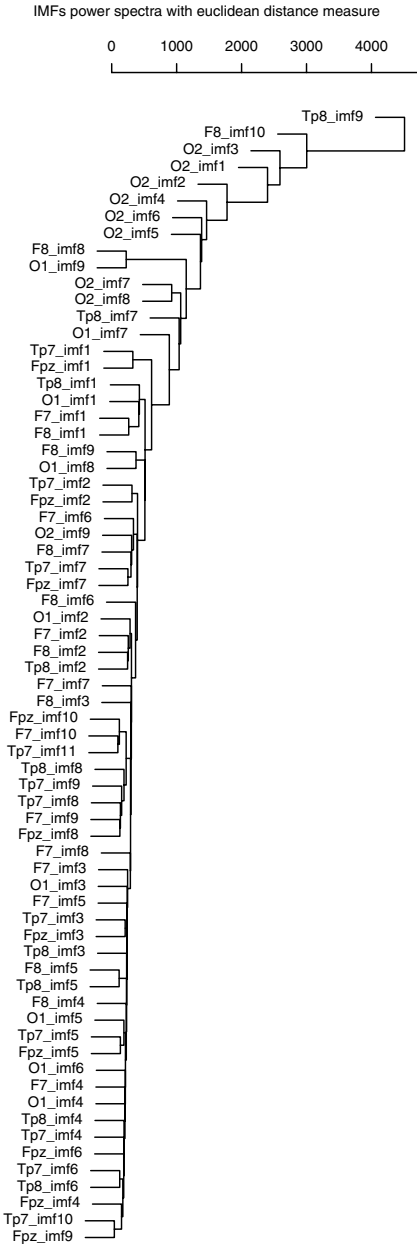
Canberra distance is calculated as

$$d_C = \sum_i \frac{|x_i - y_i|}{|x_i + y_i|}, \quad (8)$$

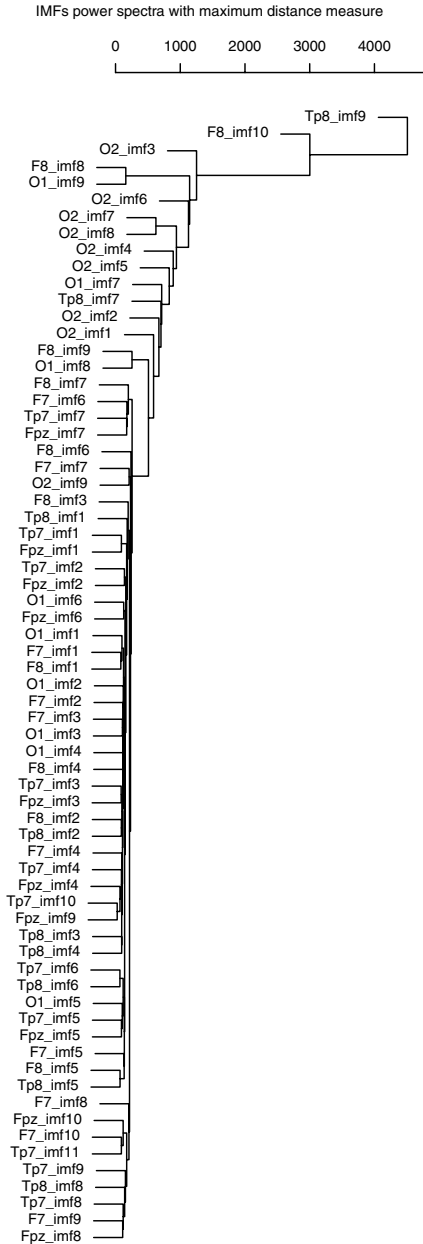
with terms with zero numerator and denominator omitted from the sum and treated as if the values were missing. A result of clustering with this measure (here the result is more interesting but unfortunately again low frequency components were mixed with those of higher frequencies) is presented in Fig. 3(b).

2.4.5. Minkowski distance

Minkowski distance is calculated as the p -norm, which is the p th root of the sum of the p th powers of the differences of the components. A result of clustering with this



(a) Euclidian



(b) Maximum

Result of the cluster analysis in form of a cluster dendrogram

Result of the cluster analysis in form of a cluster dendrogram

Fig. 2. IMF spectral clustering results for Euclidian and maximum distances methods.

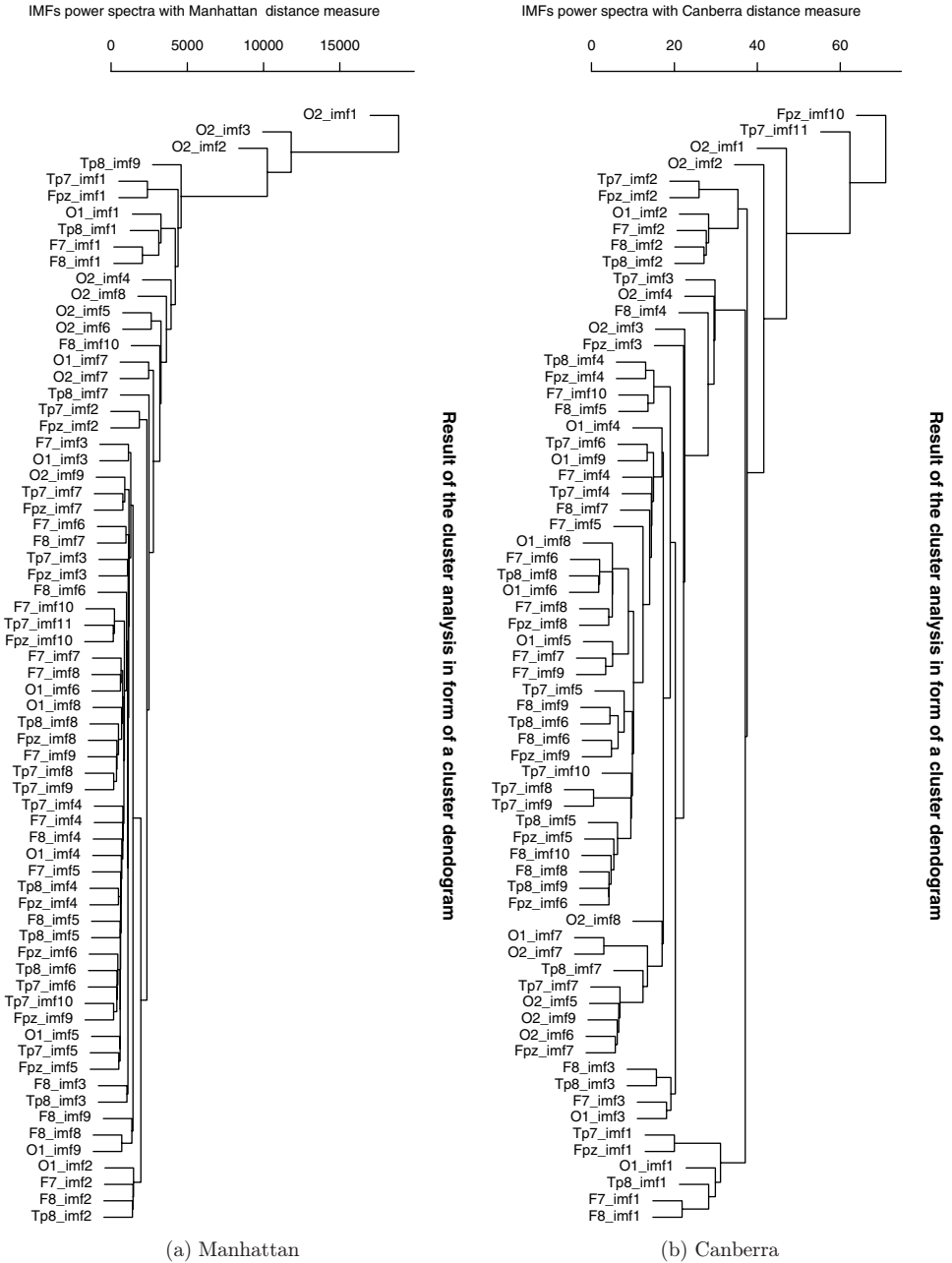


Fig. 3. IMF spectral clustering results for Manhattan and Canberra distances methods.

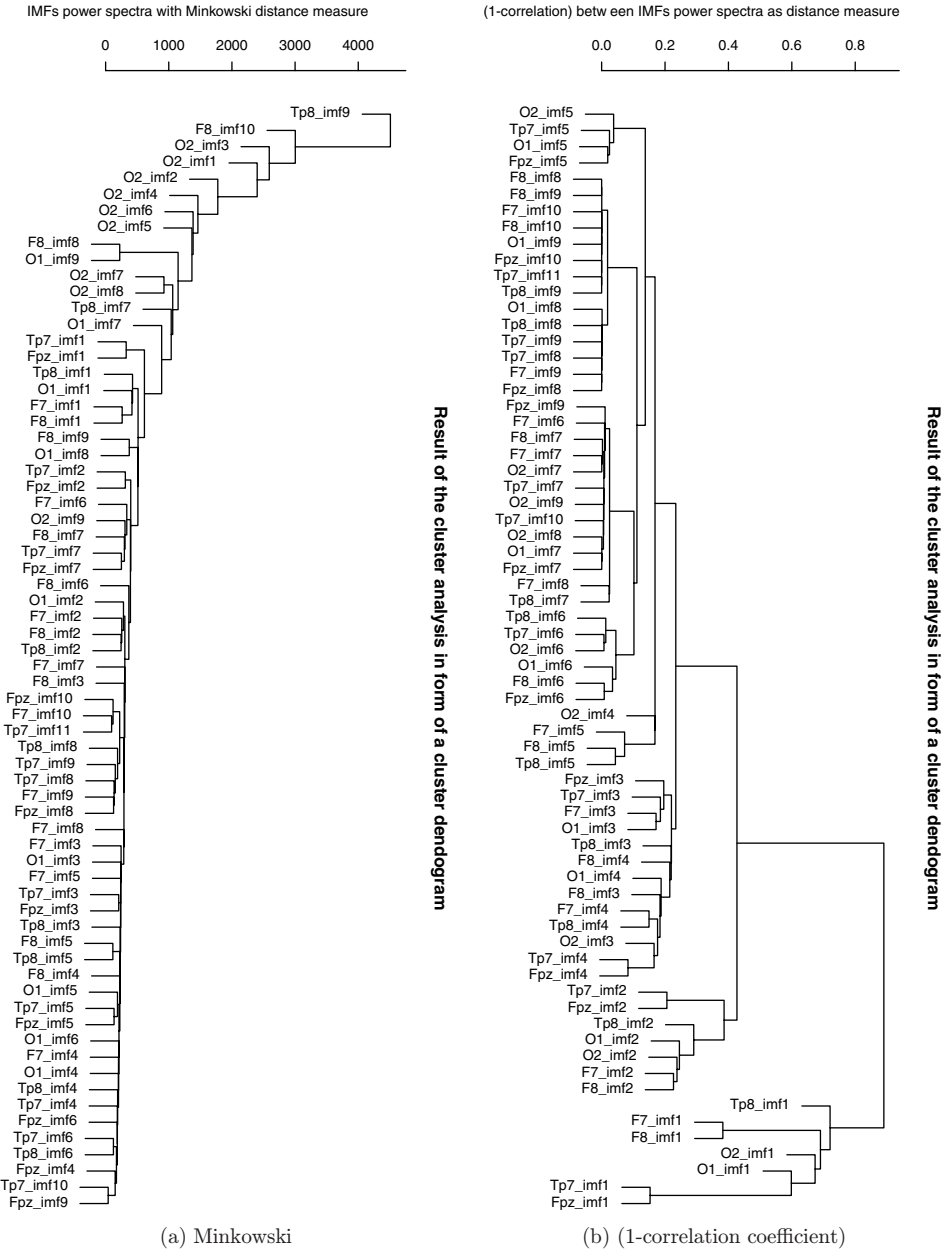


Fig. 4. IMF spectral clustering results for Minkowski and (one-minus-correlation coefficient) distances methods.

measure (here as the result again the low frequency components were mixed with those of higher frequencies which) is presented in Fig. 4(a).

2.4.6. (One-minus-correlation) distance

One-minus-correlation distance is based on correlations between vectors x and y evaluated “as a distance measure”. This result presented in Fig. 4(b) is the most interesting, since it allowed us to separate two sets of clusters.

For the best result of correlation distance measure the first set is for distances below 0.15 and those components from different channels are classified as broad-spectrally very similar and originating from nonstimuli related brain sources. The visualization of the remaining IMFs is presented in Fig. 5 and it vividly confirms the strength of the proposed method. The remaining set of clusters with distances below 0.15 was rejected.

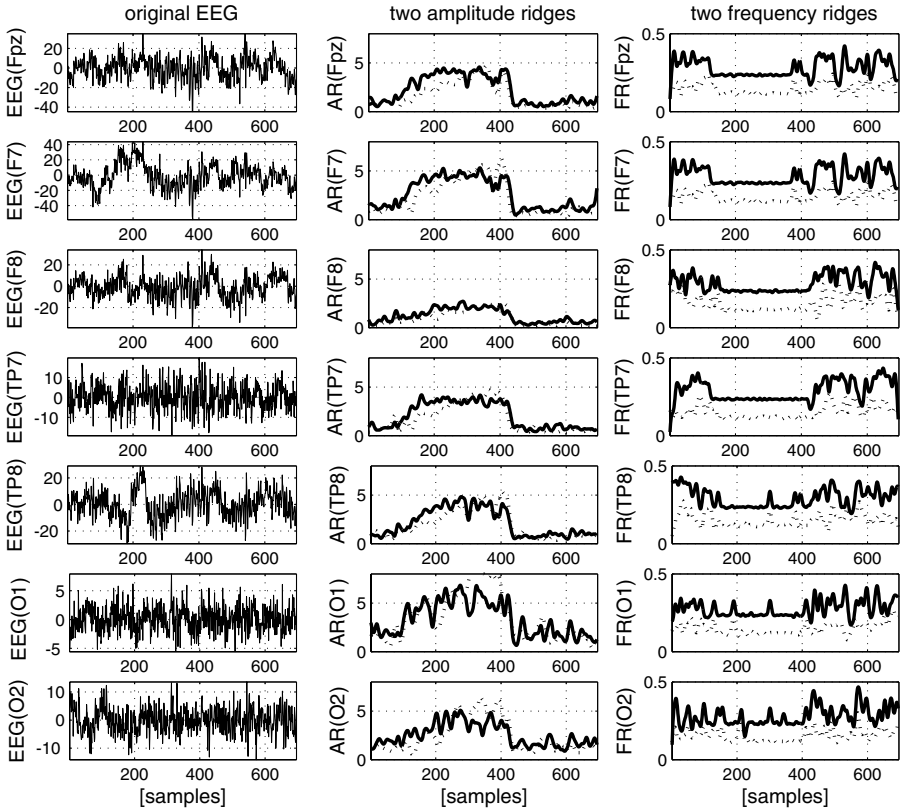
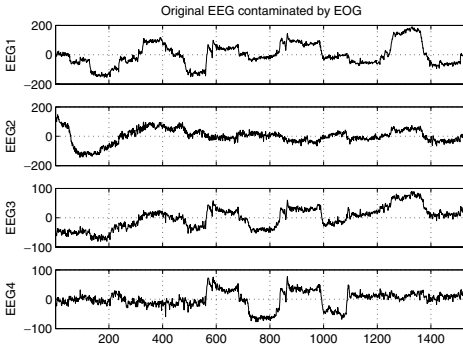
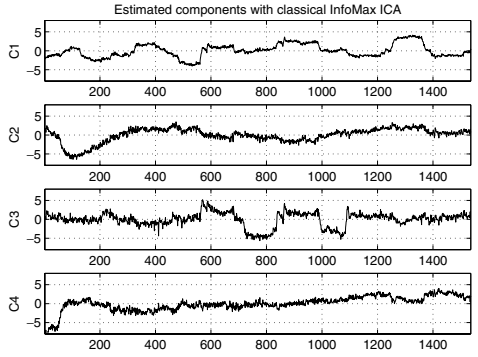


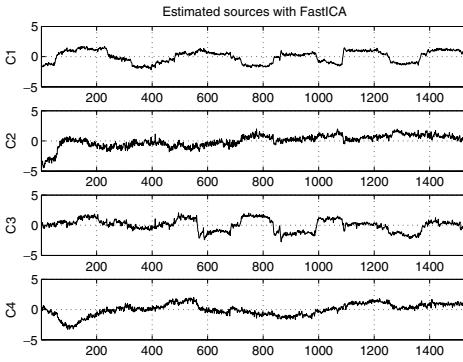
Fig. 5. The result showing the power of the proposed method to analyze multichannel EEG recordings. The first column shows noisy EEG signals, while the second and third columns depict only amplitude (AR) and frequency (FR) traces of components synchronized with the stimuli and subsequently correlated among channels (solid line for the first and dashed line for the second IMF synchronized with the stimuli).



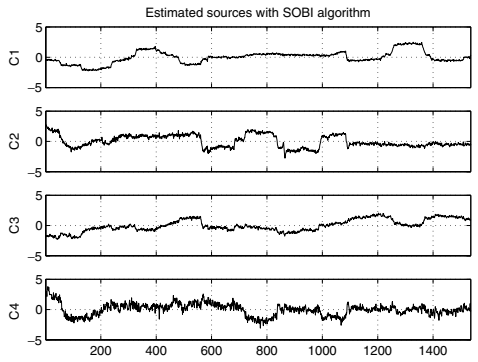
(a) Original EEG contaminated by EOG



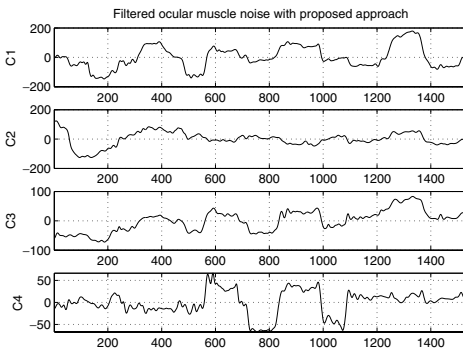
(b) Classical ICA



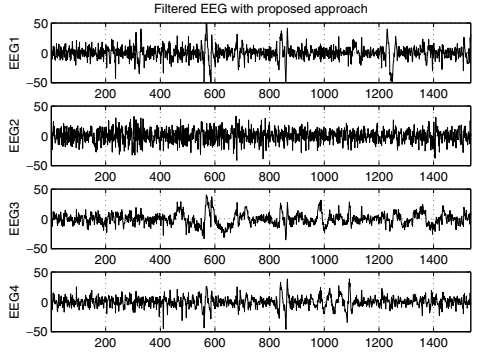
(c) FastICA



(d) SOBI



(e) EMD & clustering: EOG filtered out.



(f) EMD & clustering: recovered EEG only.

Fig. 6. Comparison of contemporary blind separation algorithms in panels (b)–(d) with the proposed approach in panels (e) and (f) in application for ocular muscle interference (EOG) removal from EEG. The original contaminated EEG signals are presented in panel (a).

3. Conclusions

An automatic framework to separate interfering stimuli related responses within EEG has been presented. This has been achieved by proposing a novel EEG decomposition technique, which allows a flexible sub-band signal decomposition while preserving the nonlinear and nonstationary features of the signals which is very crucial for brain activity analysis. The so-obtained components from each EEG channel processed separately have been further transformed to the Hilbert domain and compared within amplitude and phase domains using the clustering technique in order to identify those similar (spectrally correlated) across channels.

The resulting reconstruction has allowed us to separate common nonstimuli related EEG subcomponents from the target (stimuli related) brain activity in the data-driven signal processing approach without information leakage between channels. The proposed approach was tested in several EEG recording sessions in a multiple subjects confirming the results presented here.

For a comparison we included results with contemporary blind source separation algorithms such as classical ICA¹¹ in Fig. 6(b), FastICA¹² in Fig. 6(c), and SOBI¹³ in Fig. 6(d). These contemporary methods were not able to separate strong ocular muscle interference (EOG) from neurophysiological signals (EEG) (compare original recordings in Fig. 6(a)). The proposed approach was able to separate ocular artifacts, without additional scaling problems what was an issue occurring in the other compared approaches. The EMD-based technique presented in this paper was able to separate EOG interference (see Fig. 6(e)) from target pure EEG (see Fig. 6(f)) preserving scaling and shape distortion (compare with Fig. 6(a)). The strength of the proposed technique is based on adaptive filtering design in the completely data driven approach.

This is a step forward in EEG signal processing applications which could be useful primarily for creating user friendly BMI that would be flexible, adaptive, and response automatic detection focused resulting in fast estimation of user attention to the stimuli.

Acknowledgments

This work was supported in part by JSPS and Royal Society under the Japan-UK Research Cooperative Program, 2007 & 2008 and AOARD grant “Brain Signal Processing for the Study of Sleep Inertia”.

References

1. T. M. Rutkowski, F. Vialatte, A. Cichocki, D. Mandic and A. K. Barros, Auditory feedback for brain computer interface management — An EEG data sonification approach, *Knowledge-Based Intelligent Information and Engineering Systems*, Lecture Notes in Artificial Intelligence, Vol. 4253 (Springer, Berlin & Heidelberg, 2006), pp. 1232–1239.

2. T. M. Rutkowski, A. Cichocki, A. L. Ralescu and D. P. Mandic, Emotional states estimation from multichannel EEG maps, *Advances in Cognitive Neurodynamics ICCN 2007 Proceedings of the International Conference on Cognitive Neurodynamics*, eds. R. Wang, F. Gu and E. Shen, Neuroscience (Springer, Berlin & Heidelberg, 2008), pp. 695–698.
3. T. M. Rutkowski, A. Cichocki and D. P. Mandic, EMDsonic — An empirical mode decomposition based brain signal activity sonification approach, *Signal Processing Techniques for Knowledge Extraction and Information Fusion*, Information Technology: Transmission, Processing and Storage (Springer, 2008), pp. 261–274.
4. J. R. Wolpaw, N. Birbaumer, D. J. McFarland, G. Pfurtscheller and T. M. Vaughan, Brain–computer interfaces for communication and control, *Clin. Neurophysiol.* **113** (2002) 767–791.
5. N. Huang, Z. Shen, S. Long, M. Wu, H. Shih, Q. Zheng, N. C. Yen, C. Tung and H. Liu, The empirical mode decomposition and the Hilbert spectrum for nonlinear and non-stationary time series analysis, *Proc. Math. Phys. Eng. Sci.* **454** (1998) 903–995.
6. S. P. Kelly, E. C. Lalor, C. Finucane, G. McDarby and R. B. Reilly, Visual spatial attention control in an independent brain–computer interface, *IEEE Trans. Biomed. Eng.* **52** (2005) 1588–1596.
7. E. Niedermeyer and F. L. Da Silva (eds.), *Electroencephalography: Basic Principles, Clinical Applications, and Related Fields*, 5th edn. (Lippincott Williams & Wilkins, 2004).
8. A. W. Przybyszewski and T. M. Rutkowski, Processing of the incomplete representation of the visual world, *Issues in Intelligent Systems Paradigms*, eds. O. Hryniewicz, J. Kacprzyk, J. Koronacki and S. Wierzchon, Problemy Współczesnej Nauki — Teoria i Zastosowania — Informatyka (Akademicka Oficyna Wydawnicza EXIT, Warsaw, Poland, 2005), pp. 225–235.
9. F. Murtagh, Multidimensional clustering algorithms, *COMPSTAT Lect.* **4** (1985).
10. R Development Core Team, *R: A Language and Environment for Statistical Computing*. (R Foundation for Statistical Computing, Vienna, Austria, 2008), <http://www.R-project.org>.
11. S. Makeig, A. Bell, T.-P. Jung and T. Sejnowski, Independent component analysis of electroencephalographic data, *Information Processing Systems*, Vol. 8, eds. D. Touretzky, M. Mozer and M. Hasselmo (MIT Press, Cambridge, MA, 1986), pp. 145–151.
12. A. Hyvärinen, J. Karhunen and E. Oja, *Independent Component Analysis* (John Wiley & Sons, 2001).
13. A. Belouchrani, K. Abed-Meraim, J.-F. Cardoso and E. Moulines, A blind source separation technique using second-order statistics, *IEEE Trans. Signal Process.* **45** (1997) 434–444.